31TH EUROPEAN ROTORCRAFT FORUM
FLORENCE, ITALY – SEPTEMBER 13-15, 2005
PAPER 118

ABC ROTOR BLADES: DESIGN, MANUFACTURING AND TESTING

Henning Mainz, Berend G. van der Wall[1] (DLR)
Philippe Leconte[2], Frederic Ternoy[3], Hugues Mercier des Rochettes[3] (ONERA)
[1] Braunschweig, Germany; [2] Chatillon, France, [3] Lille, France

Abstract

ABC is the acronym for ''Active Blade Concept'' and represents a 38% Mach scaled model rotor of the Advanced Technology Rotor (ATR) of Eurocopter Germany (ECD, [4]). In contrast to the ATR the model rotor is fully articulated. Specifically, it is equipped with a flap at the trailing edge of each blade, which is driven by a piezoelectric actuator. The ABC project is a cooperation between the French ONERA and the German DLR within the research concept ''The Active Rotor''. This rotor will be used for investigations of the effect of different flap positions on noise, vibrations and performance. ONERA was responsible for the structural design of the blade and the manufacturing of a prototype blade.

DLR's responsibilities covered manufacturing of carbon fibre moulds and the five series blades (including one spare blade) using the experiences of the prototype blade manufacturing. Additionally, all instrumentation with Kulite pressure sensors, strain gages, hall sensors and accelerometers was part of DLR's contribution. In 2005 a wind tunnel test in S1MA is scheduled under the lead of ONERA with validation of the flap efficiency for vibration reduction and performance enhancement. Following this, a second test under the lead of DLR is planned in the large low-speed facility of DNW with emphasis on flap effectiveness to reduce noise radiation.

This paper deals with the particularities of the mould, the build up of the blades including the mechanism to drive the flaps, the test of the flap units in laboratory and in the S3MA wind tunnel, the manufacturing of the prototype blade and its testing and the series blades manufacturing and laboratory test of these.

The ABC Project

The ABC project [1] aims to evaluate the benefits of active trailing edge flaps mounted on the blades of the main rotor of a helicopter. Two concepts (referred to as direct-lift flap and servo-flap) were at first considered. The second one, using a small chord flap and relying on aerodynamic pitching moment to trigger blade torsion, was finally preferred.

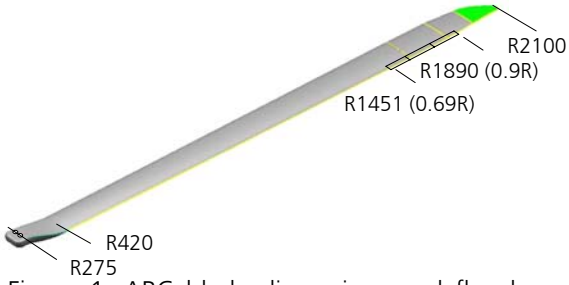


Figure 1: ABC blade dimensions and flap locations

The diameter of the Mach scaled rotor is R = 4.2m. The maximum blade chord is c = 140mm. The flap length is l_f = 0.1R in span and c_f = 0.15c in chord. Significant vibration and noise reductions have been calculated with ONERA numerical simulation codes and expected for three span wise locations of the flap**, Figure 1**.

Design of the blade

Blade geometry
The ATR blade geometry was chosen for the model rotor in order to support the full-scale investigations of industry [4]. The major difference is that the model rotor is articulated while the full-scale ATR is a hingeless rotor hub. Therefore, the blade dynamics differ, but the blade geometry and airfoils are the same.

Blade parts
The blade is made up of four main parts:
- blade root area from 0.131R, fastening section for the articulated hub, to 0.2R, first aerodynamic section;
- current section, from 0.2R < r < 0.69R;
- sections in flap area, from 0.69R to 0.9R;
- sections at tip, from 0.9R to R.

Blade root area (from 0.131R to 0.2R)
The blade root **(Figure 2**) includes the following elements.
- The main skin, of a thickness of 2.16mm, consisting of 1.54mm of current carbon rear

skin and 0.62mm of glass reinforcement woven.

- The fastening is made up of two metallic casings around which the two windings of glass roving constitute the main spar. The intermediate volume between each of four strands is filled in with right prism made of glass roving.
- Two additional glass spars (each located respectively on lower and upper inner surfaces) sit on main spar rear part and extend till the flap area sections, only the upper part extending till the tip.

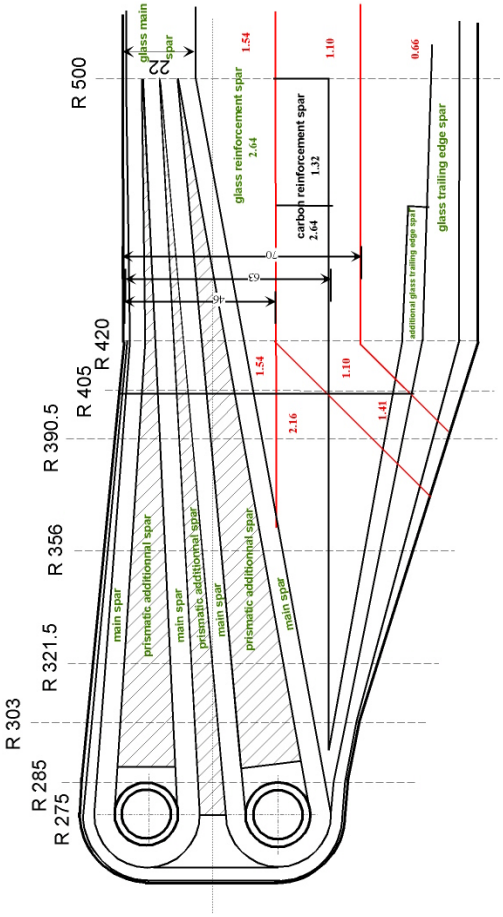


Figure 2: Blade root

- For increasing stiffness in the root area, two other reinforcement spars made of carbon uni-directional (UD) were added. The trailing edge spar starts on the front main spar, winds around the two casings and extends till the trailing edge. An additional trailing edge spar starting from the rear strand of main spar extends to the beginning of aerodynamic area.

Current section (from R420 to R1450)

The current section is presented on **Figure 3**. The skin is made of the following elements:

- a pre-cured skin on which instrumentation is implemented. This skin is made of SXM10 carbon protection woven layered at 0° and two plies of 920CTS carbon UD layered at ±45°.
- An inner skin made according to the chord of four and two plies of 920CTS carbon UD layered at ±45°,

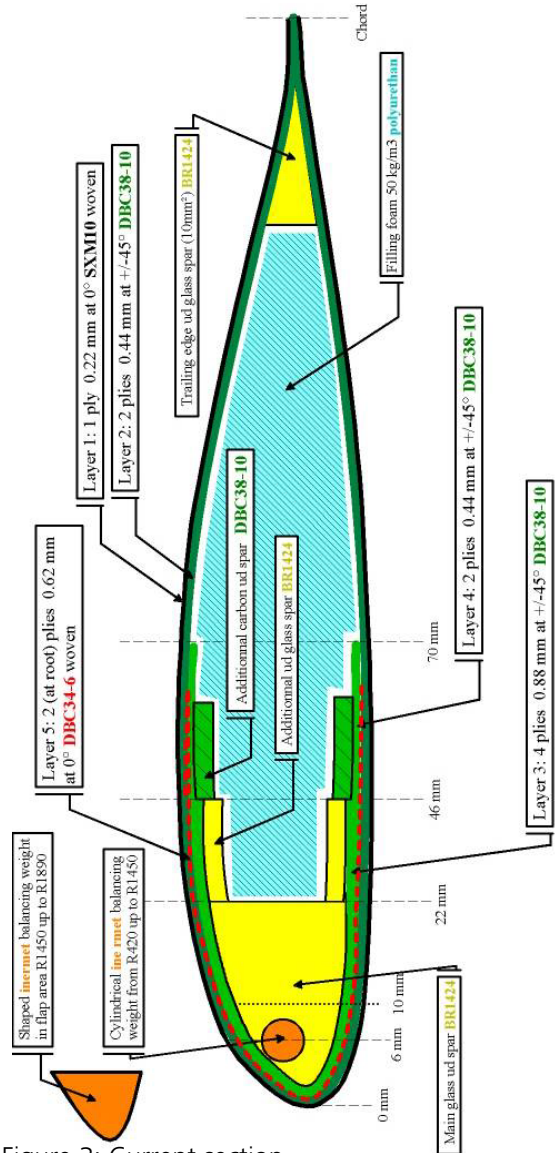


Figure 3: Current section

The internal structure is made of:

- the main pre-cured glass spar up to 22mm from leading edge ;
- between 0.2R and 0.69R tungsten balancing weights made of 4mm diameter rod and inserted / glued in a span-wise slot milled in the main spar;
- the two additional glass spars on lower and upper surfaces, 2.64mm thick and up to 46mm from leading edge;
- foam blocks of a density of 50kg/m^3 fill up the remaining volume and the trailing edge glass spar of a section of 10mm²;

- between 0.238R and 0.381R, additional lumped mass made of tungsten for minimizing the blade frequencies coupling. This mass is glued on the rear face of the main spar and on inner surface of additional glass spars.

Sections in flap area (from 0.69R to 0.9R)

The flap area is shown on **Figure 4** in perspective, viewed from bottom.

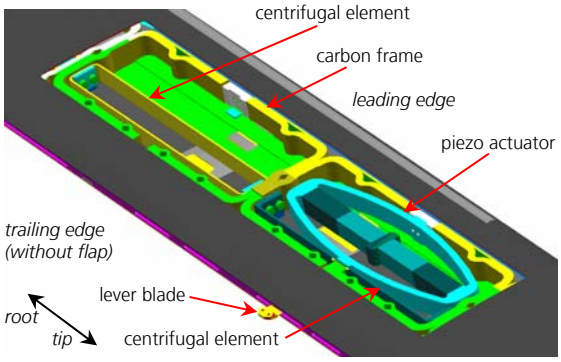


Figure 4: Flap area

The skin is the same as for the current section up to 0.721R but from 0.722R (beginning of the actuator frames) to 0.9R, the thickness changes are limited according to the carbon frame and the trap door which is located on lower surface from 0.722R to 0.88R. For the inner structure, the changes are the following:

- the lower additional glass spar with 2.64mm thickness stops;
- the upper additional glass spar increases in chord direction up to 50mm with respect to leading edge and thickness decreases down to 0.88mm;
- the lower additional glass spar ends;
- the balancing weight made of tungsten is implemented at leading edge, shaped up to 10mm with respect to leading edge and glued on front of the machined main spar;
- actuator frame consisting of an internal twin frame and an external frame made of high modulus carbon UD is glued on rear face of main spar;
- according to the flap configuration, the actuator is clamped on a metallic insert implemented inside the rear area of main spar;
- moving flaps are clamped and/or inserted in a slot on the rear area of the external frame by means of hinge blades and fixed flap by means of heel.

Sections at tip (from 0.9R to R)

The blade tip area is made of the following parts presented on **Figure 5**.

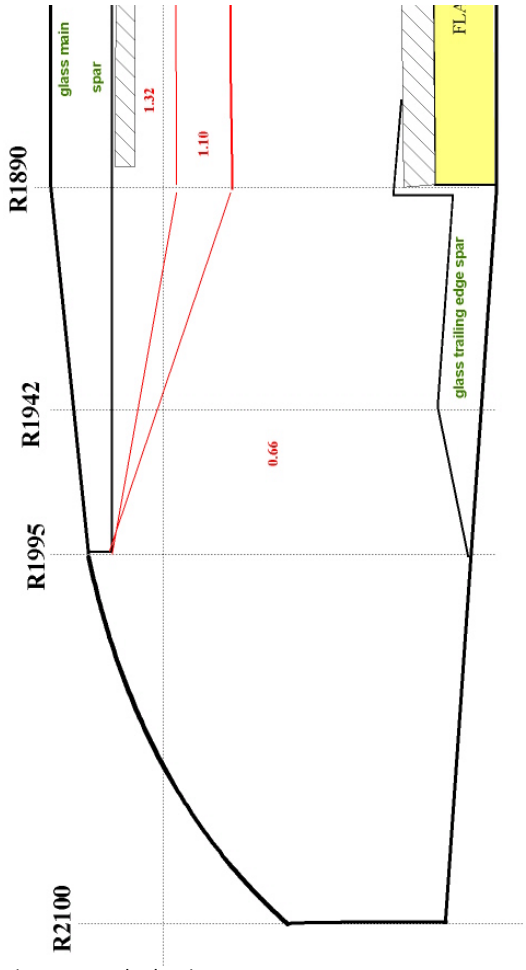


Figure 5: Blade tip

The skin is the same as for the flap area section starting from 0.9R but the limits on the thickness of the inner skin layers and corresponding changes are the following in the parabolic tip area:

- the four plies are changed in three plies limited at 36mm in chord extended straight ahead in span direction on rear spar at 0.95R;
- the two plies are limited at 50mm in chord and extended straight ahead in span direction on rear spar at 0.95R;
- main spar ends at 0.95R;
- filling by 50kg/m^3 foam and at R on 10mm by carbon woven to ease the trimming of the blade length.

Blade manufacturing process

The blade manufacturing can be summarized by the following basic process:

- pre-curing of external skins (3 layers) with pressure sensors inner protection woven;
- milling of woven inner stands for pressure sensors housing;
- gages, sensors and wires implementation;

- separately layering and curing of a rough main spar;
- shape-machining of the raw spar front area with the balancing weights at leading edge;
- machining of spar slot for implementation of balancing cylindrical weight;
- manufacturing of pre-cured actuator composite frames and shape-machining of these parts;
- assembling and gluing of carbon frames on main spar by using an assembly jig with dummy interfaces (dummy flap, dummy lever blades, dummy actuators;
- layering of others inner components (uncured inner skins, reinforcement spars, trailing edge spar, foams, …) together with the assembling;
- curing of blade with dummy flap;
- actuator trapdoor milling on final blade;
- driving out of assembling and dummy flap;
- trap door layering on specific mould;
- assembly of the flap actuator components.

Blade instrumentation

The blade instrumentation is carried out as follows:

- Pressure sensors are implemented on upper and lower surfaces of blade as well as in fixed and moving flaps (blade 1 to 4). Pressure sensors distribution is presented on **Table 1** where: A (Kulite LL-32-072-25-A) is a sensor with pipe, Aq (Kulite LL-32H-072-25-A) is a A with thermal compensation and B (Kulite LL-072-25-A) is a sensor without pipe;
- Strain gages bridges (Vishay CEA 06 125 UN 350Ω) for SPA blade deflection measurement implemented on blade 2 and 5;
- Strain gages bridges (Vishay CEA 06 125 UN 350Ω), for fatigue monitoring, implemented on all blades at the critical section and on a root section;
- Two tip accelerometers (Endevco Isotron 25A) for deflection checking on blade 2;
- Hall effect sensors for flap angle measurement located on each moving flap tips. The sensors (Honeywell SS495A1) are implemented in the rear area of the carbon frame and the magnets (Honeywell 103MG5) in the leading edge of the flap.

All instrumentation wires are connected on two plugs (CANNON 2DD100S-FO) located at the trailing edge of blade root.

	# of pressure sensors
Blade 1	50A + 4B (10Aq)
Blade 2	30A + 4B (4Aq)
Blade 3	56A + 6B (8Aq)
Blade 4	30A (16Aq)
Total	166A + 14B

Table 1: pressure sensor distribution

Mechanical characteristics of blade sections

The mechanical characteristics data (19th version) of the blade sections (67 stations) are calculated for the three flap locations corresponding to two configurations:

- configuration 12-6MOD19: inboard flap and middle flap, inboard actuator;
- configuration 23-6MOD19: outboard flap, outboard actuator.

The mechanical characteristics are the following:

- R (m): radius;
- Ml (kg/m): weight distribution;
- <Eib> (N/m²): equivalent flap stiffness;
- <Eit> (N/m²): equivalent chord stiffness;
- Rholp (m.kg): distribution of pitch polar inertia sum;
- Rholpp (m.kg): distribution of pitch polar inertia difference;
- <GJ> (N/m²): equivalent torsion stiffness calculated with PATRAN/NASTRAN code [3];
- Ycdg (m): c.g chordwise location/pitch axis, positive towards leading edge;
- Ycn (m): neutral axis chord wise location/pitch axis, positive towards leading edge;

In the flap area, the stiffness <Eib>, <Eit> and <GJ> are calculated with a trap door made in one piece with the blade. These data of sections for inboard configuration are plotted on Figures 6 to 9 on the following side. They take into account the following mass elements:

- two couples (male and female) of instrumentation plugs at root;
- flap actuator components (hinge blades, lever blade, centrifugal blades, screws, pins, …);
- inner composite stands of pressure sensors.

The fan diagrams of the mod19 versions of the blade, respectively with actuator in position 12 and 23, are presented on **Figure 10**.

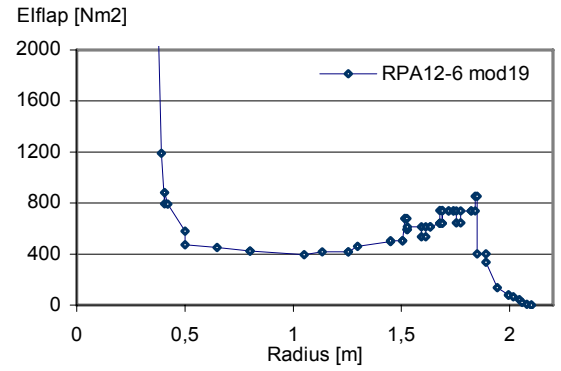


Figure 6a: flap stiffness

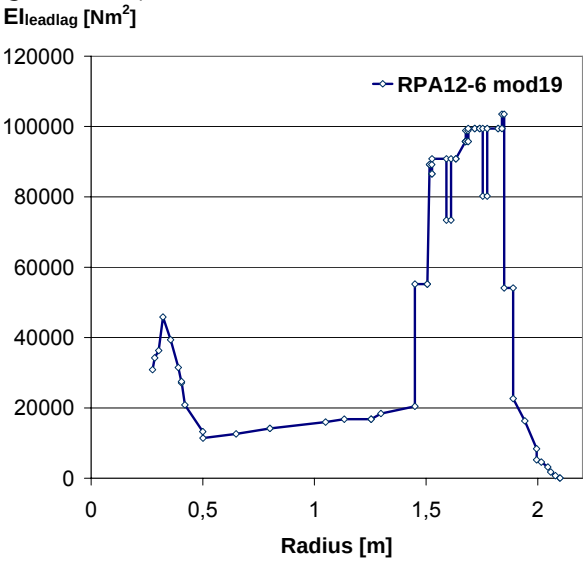


Figure 6b: lead-lag stiffness

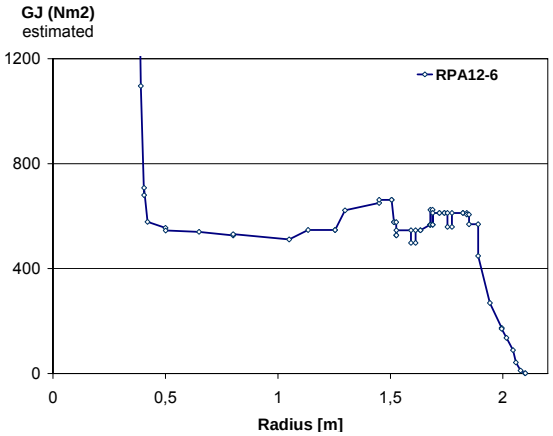


Figure 6c: torsion stiffness

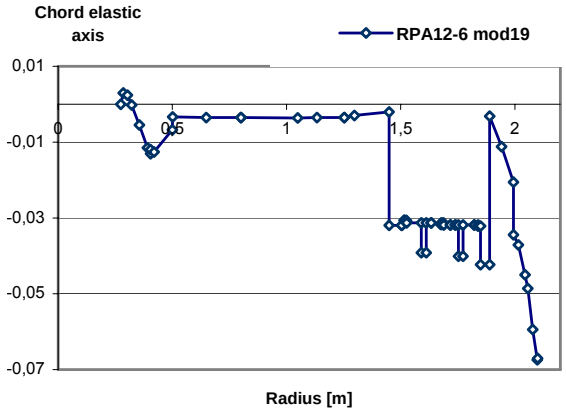


Figure 7: elastic axis position

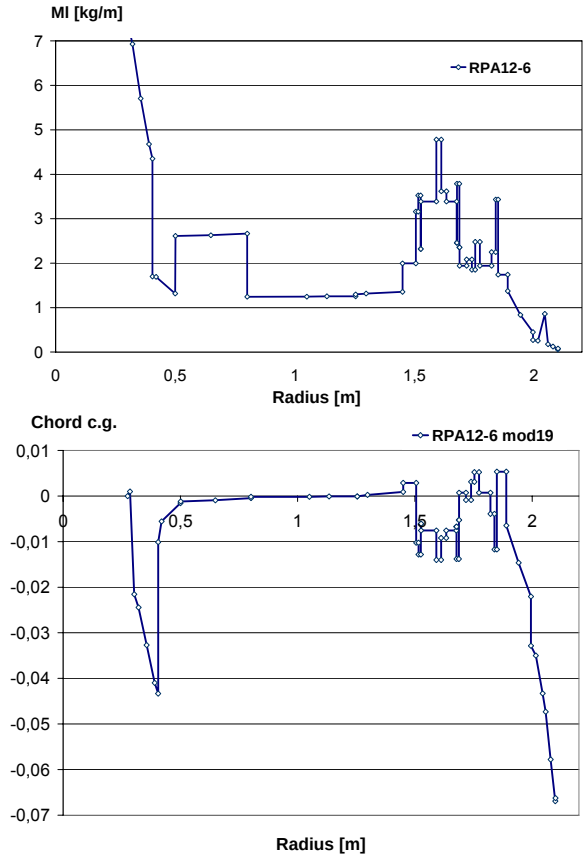


Figure 8: mass distribution (top), mass axis (below)

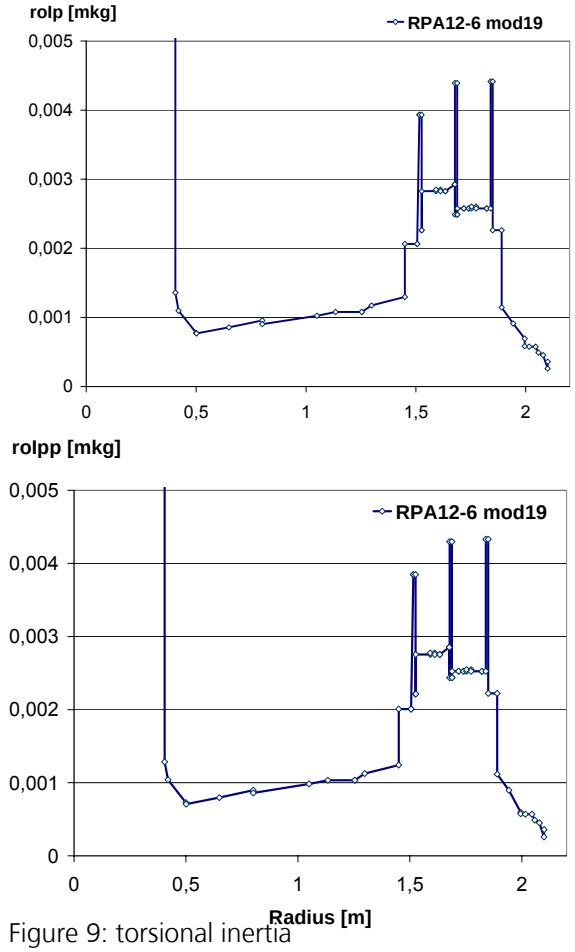


Figure 9: torsional inertia

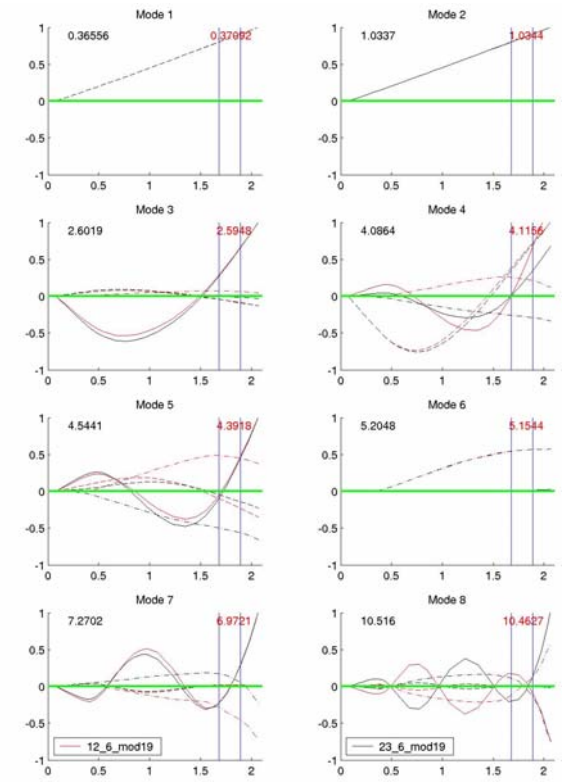


Figure 10: Fan diagram, mod19 version

Design and manufacture of Flap Actuator device

The piezoelectric actuator used to deflect the flap, located inside the blade model, is an APA500 manufactured by the French company CEDRAT Technologies. This actuator features four stacks made of soft piezoelectric ceramic which are located and pre-stressed on the major axis of an elliptic steel shell. When a positive voltage is applied to the stacks their length increases and the minor axis of the elliptic frame decreases with a stroke ratio of about 5.2.

The power amplifier used to supply the actuator is a LA75C made by CEDRAT and limited to a voltage of -20/+150V and 2.4A driving current. Some of the nominal characteristics of the CEDRAT APA 500 elliptic actuator are presented in the **Table 2** below.

Maximum stroke	500µm
Blocked force *(pulling or pushing)*	570N
Rigidity	1.14N/µm
Natural frequency (blocked-free)	460Hz (nominal) 485Hz (measured)
Maximum supply voltage	-20V to +150V
Capacity	40µF
Quasi-static resolution	0.05µm
Mass	200g

Table 2: Actuator properties

Flap actuator device description

The basic concept of the flap deflecting device is to actuate the 15% chord flap with one elliptic piezoelectric actuator alternatively located at 0.763R, or 0.84R from the rotor axis and according to the flap configurations (see **Figure 4**). Three different moving flap elements are used depending on the span wise position at which the active flap is to be studied on the blade (this is due to the planform of the blade). Corresponding fixed flap elements are used to ensure the blade planform continuity when the flap is transferred from one position to another. Each moving flap element is driven by one actuator:

- flap unit inboard from 0.69R to 0.8R, length 229mm (actuator position 1-2 at 0.763R);
- flap unit in middle from 0.746R to 0.855R, length 229mm (actuator position 1-2 at 0.763R);
- flap unit outboard from 0.8R to 0.9R, length 210mm (actuator position 2-3 at 0.84R).

The flap geometry design from 0.69R to 0.9R has been chosen as a compromise with respect of conflicting constraints: the blade is twisted, the rear part of the frame along span must be a plane parallel to the rear of the spar to simplify the frame manufacture, hinge blades along span must be a plane to allow their deflection in good

conditions, flap with 15% chord (small size) and flap rotation axis located at mid-thickness.

The flap geometry along span is summarized in the following **Table 3**.

r/R	0.69	0.76	0.8	0.83	0.86	0.9
c_f/c	0.12	0.15	0.15	0.15	0.15	0.15
Flap location axis, upper surface, %	51.8	50.6	50	50	51	53

Table 3: Flap geometry

Mainly based on the first configuration described before, a prototype made of aluminium of 140mm of chord was designed, manufactured and tested in S3 Modane blow-down wind-tunnel and in centrifugal field on BRAVoS hover test rig **[1]**.

The flap presently implemented in the blade model has been strongly inspired from this metallic prototype, although some difficulties were encountered adapting the design to the use of composite materials **[2]**.

A block of surrounding frames is devoted to stiffen the flap area and is made of an internal frame to secure the trap door on lower surface and an external frame allowing the connection between the spar and the flap-blade interface.

Each elliptic actuator is clamped on one side on the rear of the main spar by means of a metallic insert which is inserted and glued into the spar.

On the other side, the actuator is clamped on a double centrifugal blade to withstand the overhang produced by the centrifugal field and to prevent any parasitic vertical displacement of the actuator. The two ends of this centrifugal blade are screwed on the surrounding rectangular carbon frame. In configuration 2-3, with the actuator at the most outboard position, an additional centrifugal blade made of carbon roving is implemented in the inner actuator location.

The actuator deflects the flap by means of fork joint on which is clipped a lever blade made of steel. Between the centrifugal blade and the lever blade, a wedge can be installed to trim the neutral flap angular position (without power supply). The flap can turn around a pseudo-axis defined by the deformation in flexion of composite hinge blades. These blades are located on both sides of the lever blade in the span wise direction and inserted on one side in the moving flap and clamped on the other side in the external trailing edge frame. The fixed flaps are clipped in the frame by means of a nut with the same fasteners as those of the moving flaps.

All flaps are moulded in carbon woven composite soaked with a cold process laminating resin.

The innovative linkage between the flap and the piezoelectric actuator presents several advantages:

- no friction: calculations including the radial and centrifugal loads with 4 bearings give, according to the kind of surface treatment (graphite or molybdenum bisulphide), a friction moment between 29% and 47% of the actuator maximum moment. With thrust bearings, these values can be decreased to between 8% and 12% but there is no room for such a kind of bearings, no local wear since the cinematic is ensured by elastic deformation and no mechanical play. Since the stroke of the actuator is rather small, not the slightest part of it should be wasted. Furthermore, the transfer function between the actuator and the flap must be as limited as possible to enable an easy control of the flap;
- the centrifugal force generated by the flap mass is withstood by the hinge blades along the full span of the flap (a flap of 420mm span gives about 1600N when rotating at 115rad/s);
- limited elastic resistant moment of the hinge blades whatever the centrifugal field might be (5% of the actuator moment with hinge blade made of two glass composite layers, 13% with three layers);
- good fatigue behaviour, as preliminary calculations on the hinge blades (two layers at 0°) give a fatigue margin of 1.27;
- simplicity of assembling since no fitting and no rotation axis are required;
- easy maintenance as no greasing is required;
- in case of cracks developing on lever blade and/or along hinge blades, these would be visually easily detected during periodic checks made after each rotation sequence in the wind-tunnel;
- light mass of the flap/blade hinge when compared to more conventional bearings;
- high natural frequencies estimated between 150 and 200Hz according to the type of setting. The frequency of OA312 section prototype is up to 160Hz;
- the hinge blades located all along the flap span could have a beneficial effect with respect to aerodynamic sealing between upper and lower surfaces of the blade **[2]**.

In spite of all these advantages, some drawbacks have to be overcome:

- due to the use of hinge blades instead of a more conventional axis design, the equivalent rotation axis slightly moves fore and aft during the flap deflection. This movement depends on the flap angle, the stiffness of the hinge blades and the operating frequency;

- for similar reasons, the accurate flap angular position measurement is not easy;
- the connecting device between the actuator and the flap can be seen as a reversible system (depending on its intrinsic stiffness);
- the natural characteristics of such a piezo actuator: rather heavy unit mass, hysteresis, part of energy lost in the pre-stress loading of the system, one-way actuation mode of operating, balance between stroke and blocking force.

Starting from the performances measured on the blade section prototype **[1] [2]**, the expected characteristics of flap actuator device in blade model are presented in **Table 4**.

Lever blade	material	Steel Marval 18
	Thickness	0.3 mm
	width	10 mm
Hinge blade	material	2 plies GFRP at ±45°
	Thickness	0.26 mm
	Elastic length	5 mm
Centrif. blade	material	Steel Marval 18
	Thickness	1 mm
	Elastic length	twice 63 mm
	width	10 mm
Actuator distance lever blade/hinge blade		1.60 mm
	Voltage supply	-20 to 150 Volts
	Angular stroke	0-13°
	Angular position	-4.5° (150V) to 8.5°(-20V)
	Stiffness	0.092mN/°
	Blocking moment	1.2 Nm
	Natural frequency	160 Hz

Table 4: Expected flap drive system characteristics

Prototype blade tests

Lab tests

The blade prototype was tested in lab with respect to the performance of the flap actuator for the three flap configurations and shows (see **Table 5**) an angular stroke lower than that (up to 12°) obtained with flap unit section prototype made of aluminium described before.

Flap configuration	Inboard flap	Central flap	Outboard flap
Flap angle (peak to peak, -20V/+150V)	9.65°	8.76°	9.23°

Table 5: Flap stroke

Mass and cg were measured (see **Table 6**) and comparison with calculation shows a good correlation.

Parameters	Actuator inboard		outboard	
	Tests	Calc.	Tests	Calc.
Mass (g)	3878	3959	3886	3977
Static Momentum (mkg)	3.900	4.005	3.951	4.076
Rcg (mm)	1005.8	1011.8	1016.6	1025.0
Chord cg /25%	-4.6 back	-7.5	-6.4	-7.6

Table 6: Calculated and measured masses

Wind tunnel tests

The blade prototype was tested in non-rotating mode in S3 Modane wind tunnel where one of the objectives of the test was to validate the flap actuator behaviour under aerodynamic loads. The blade was mounted on a specific device, while the flap was in the inboard area close to the right wall as shown on **Figure 11**. The device allows varying statically or dynamically, the angle of attack of the blade.



Figure 11: Prototype blade in wind tunnel

Static tests with zero angle of attack were performed at four Mach numbers, in open loop and for three voltages applied on actuator corresponding to flap up (negative angle), flap at zero and flap down. Results presented on **Figure 12** shows that at increasing Mach numbers the angular stroke is decreasing and slightly more for negative angle. Flap angle is changing from 9.8° without wind to 6.4° at Mach 0.65 and to 5.3° at Mach 0.8 with a shift in direction of negative angle.

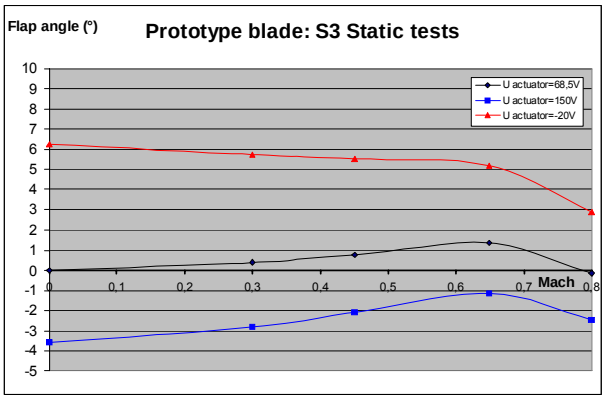


Figure 12: Static tests

Series Blades

Mould

Before giving some information concerning the mould it requires to have a look at the design of the blades and especially the kind of fibre materials used. As mentioned above the blades consist of several pre-cured and milled parts (skins, spar, frame). These parts were assembled together with some uncured fibre layers and milled foam blocks which fill the cavities. For most of the parts prepregs were used. Prepreg means already with resin impregnated fibre material.

The particularity and the big disadvantage of prepregs in our case is that they have to be cured at round about 120°C. A lot of millings have to be done during the blade manufacturing process. Therefore it is necessary that the skins and the raw cured blades fit perfectly into the mould. Consequently the different thermal expansions of potential mould materials have to be considered. **Table 7** shows some guide values of the thermal properties of different materials.

	Thermal expansion [• 10^{-6}/K]		
Material		II filaments	⊥ filaments
Aluminium	23		
Steel	14		
Glass fibre		6,5	22
HT carbon fibre		0	29
HM carbon fibre		-1,2	34
Invarsteel	1,5		

Table 7: Thermal expansion coefficients

Contrary to metals, composites are anisotropic materials and the expansion of them depends first on the kind of fibre, second on the fibre volume content, and third on the layering. The values shown in **Table 7** apply for composites with a fibre volume content of about 60%. Remarkable is that high tension (HT) carbon fibre does not expand and high modulus carbon fibres even shrink parallel to the filaments if the temperature increases. Perpendicular to the filaments the thermal expansion of composites is much higher in comparison to metals. In composites which consist of several fibre layers with different filament orientations the filaments suppress the expansion so that in sum the expansion is very small.

The ABC rotor blades have a length of 1.8 meters. **Table 8** shows the calculated elongations of parts which consist of different materials if they are heated up from 20°C to 120°C.

$\Delta T = 100K$; $l = 1800$ mm
$\Delta l_{Steel} \approx 2.8$ mm
$\Delta l_{Aluminum} \approx 4.3$ mm
$\Delta l_{Glasfibrell} \approx 1.2$ mm
$\Delta l_{HMcarbonII} \approx -0.22$ mm

Table 8: Impact of thermal expansion coefficients

The experiences of the ERATO rotor blade manufacturing with a steel mould in combination with a carbon fibre skin delivered the result that standard steel or aluminium moulds are totally unsuitable for the ABC blade manufacturing. An utilisable material would be Invarsteel. This is a special steel alloy with a thermal behaviour like isotropic layered carbon fibre composites. Invarsteel moulds enables to manufacture a lot of parts without loosing the quality of the mould. Unfortunately this kind of steel is very expensive and consequently inapplicable.

We needed a mould with nearly the same properties like the carbon fibre skins of the blades and the mould should enable us to manufacture in sum six rotor blades (one prototype blade and five series blades). Thus a carbon fibre mould seems to be the solution of the problem. The thermal behaviour of such a mould should correspond to the behaviour of the skins and a carbon mould should be robust enough to allow us to manufacture the needed amount of blades. Unfortunately no construction manual was available which told us how to manufacture a "high temperature useable" composite mould.

The experiences with such kinds of moulds are either very small or secret. Thus it was necessary for us to develop our own carbon fibre mould which fulfils requirements of profile accuracy smaller than 0.1mm. A basic step of the mould development is to detect the influence of the fibre distribution and the thickness on the accuracy.

Before starting to manufacture a mould and in our case at first some test moulds it is necessary to define the way how to manufacture them. Anyway the first step is building a positive mould made of a kind of foam, of plastics or metal. Then some carbon fibre layers with resin

have to be put on the surface of this positive mould so that a negative mould results.

In general there are three ways to manufacture a composite.

- The first one is to take the fibre material and to impregnate each single layer with resin by hand using a brush. Generally this is a very effective method to obtain very good results. Usually the fibre volume content is not so high and the used resins are not high temperature resistant. Therefore this method is not so appropriate in our case.
- The second method is to use prepregs (resin pre-impregnated fibre layers).
- Third it is possible to apply the dry layers on the mould, cover them with a vacuum bag, put all things into an autoclave and inject the resin. This method is called DP-RTM [3] (Differential Pressure – Resin Transfer Moulding).

Prepreg and the DP-RTM method need a high pressure around 6bar and curing temperatures up to 150°C. Achieving fibre volume contents of about 60% is no problem. The advantages of the DP-RTM are:

- high fibre volume content
- good quality of the composite
- The layers are much thicker than prepreg layers => it is much easier to achieve the required mould thickness

Typically the thickness of prepreg layers amount between 0.1 and 0.2mm. A DP-RTM method layer is usually round about 1mm thick. **Figure 13** shows on the left side a prepreg layer with a thickness of 0.2mm and on the right side a 0.85mm thick DP-RTM method layer.

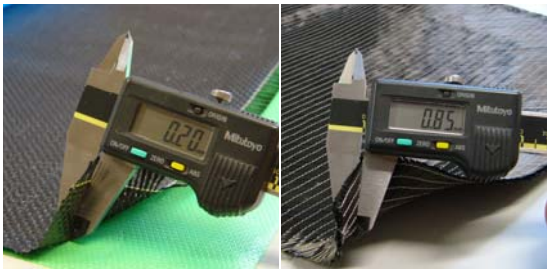


Figure 13: Carbon Prepreg and DP-RTM layer

As we used the DP-RTM for the manufacturing of the test moulds and the final ABC rotor blade moulds a description of this method is given in **Figure 14** and the following text.

The fibre material is applied in dry state to the mould. Vacuum foil covers the fibre material. The borders of the foil are bonded with a special sealing compound so that it is possible to evacuate the fibre material. After a pressure of 6bar and a temperature of 70°C inside the autoclave are applied once the vacuum line is closed. The injection starts when the valve of the injection line is open and the resin flows from the heated and pressurized resin reservoir into the fibre material. By means of a pressure reducer the pressure inside the resin reservoir is reduced about 0.2 up to 0.4bar when the resin flows into the transparent vacuum line.

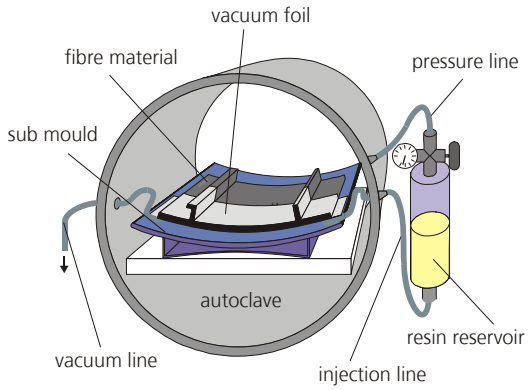


Figure 7: DP-RTM method

Fibre volume content and fluid rate can directly be controlled by adjusting differential pressure during the stages of injection. Depending on the resin used, the curing of the component usually takes place at temperature between 120°C and 180°C. **Figure 15** shows the aluminium positive test mould.

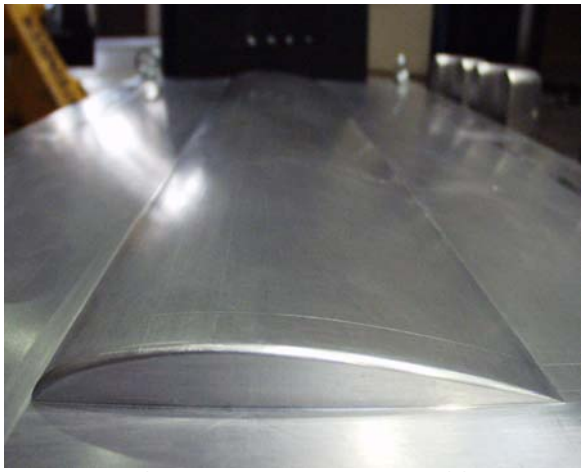


Figure 15: Aluminum positive test mould

The blade segment has a rectangular shape of 800mm length and 140mm width. The maximum thickness amounts 17mm.

A various number of parameters have an influence on the quality of the mould. For example the:

- layering
- thickness
- fibre volume content
- curing temperature
- the temperature treatment after curing

Test moulds

Figure 16 shows the first test mould. It has a thickness of about 1cm and consists of only 9 carbon fibre layers.



Figure 16: First test mould

Measurement results of one cut of the aluminium mould compared to the corresponding cut of the test moulds 1 and 3 is visible in **Figure 17** 30 times boosted.

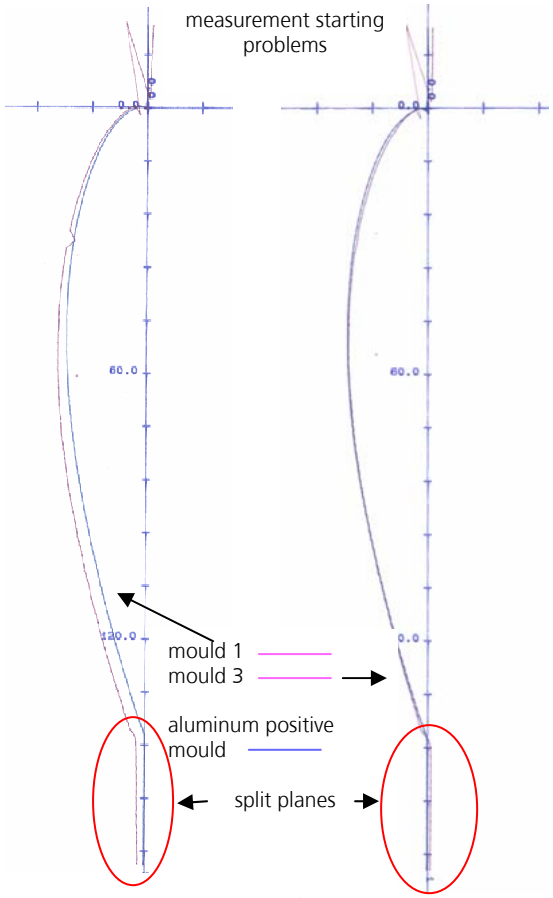


Figure 17: Measuring results

The first mould was a little bit twisted and the split planes on leading and trailing edge were not parallel. Changes of the layering and production parameters lead to mould 3. The split planes of this mould were nearly parallel, no twist is visible and the tolerances were below the specified range. Measurements of the mould length at 20°C and at 120°C confirmed the assumption that the thermal expansion of the mould perpendicular to the fibres is suppressed trough the fibres which lie parallel to this direction.

Real ABC blade moulds

The manufacturing of the real blade moulds starts with the milling of aluminium positive moulds. Aluminium is an isotropic material but unfortunately the manufacturing process causes inner tensions. These inner tensions can lead to warping in case the material is milled only one sided. **Figure 18** shows the upper side of the positive mould.

To achieve the right carbon negative mould dimension it is necessary to scale the aluminium positive mould down this way that the calculative dimension of the positive mould at the resin curing temperature (for instance 100°C) corresponds to the final required dimension.



Figure 18: One positive mould

Ignoring the different thermal expansions of aluminium (α_a = 23•10^{-6}/K) and carbon ($\alpha_c \approx$ 0•10^{-6}/K) would deliver an oversized blade. In our case (blade length l = 1800mm) the elongation of the blade length would be:

$\Delta l = l \bullet \alpha_a \bullet \Delta T$ = 1800mm•23•80K•10^{-6}/K = 3.3mm

The right side of **Figure 19** shows the final step of the mould layering before the tear off sheet and the vacuum bag are applied whereas the left mould is already evacuated. Well visible on the bottom of this figure are the copper injec-

tion lines and on the left side the plastic vacuum line.



Figure 19: Mould layering

The ABC blade moulds shown in **Figure 20** consist of 29 carbon fibre layers with different orientations and a total thickness of round about 16 mm.



Figure 20: ABC blade moulds

Series blades

The following paragraphs deal with the blade manufacturing process and ought to give an overview of the steps needed by means of pictures from the series blade manufacturing.

As already mentioned the skins of the blades are made of three prepreg carbon fibre layers with a total thickness of about 0.66mm. The carbon fibre stripes visible in **Figure 21** thicken the skins at positions where later on pressure sensor are installed.

The next step before curing the skin in the autoclave at 120°C and 4 bars is to cover the uncured skin with a tear off sheet and a vacuum foil. **Figure 22** shows a part of a skin lying in its mould. The five blades (including the spare one) are equipped with:

- 180 pressure sensors (4 or 5 wires/piece)
- 300 strain gauges (2 wires/piece)
- 30 Hall sensors (4 wires /piece)
- 2 accelerometers

=> approx. 1500 wires diameter 0.3mm were installed.



Figure 21: Uncured skin with reinforcement layers

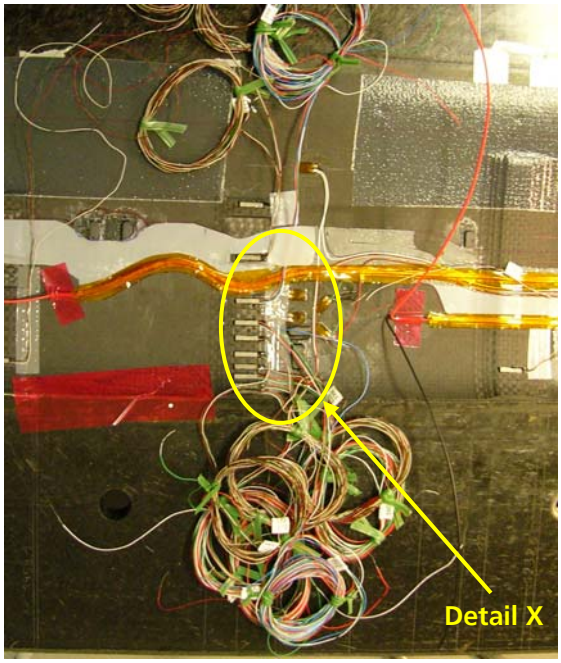


Figure 22: Skin with pressure sensors

The pressure sensors are installed into longish cavities which are milled into the reinforcement layers. **Figure 23** (detail X of **Figure 22**) shows a blow up of a pressure sensor section including the actuator power supply wires and some strain gauges which are directly glued on the skin.

Each single numbered wire had to be laid on the inner skin surface from the sensor to the grommet in root of the blade (**Figure 24**).

In case of the series blades manufacturing the wires were fixed using prepreg glue film which adheres if it is warmed as an example by means

of a soldering gun or a temperature adjustable dryer.

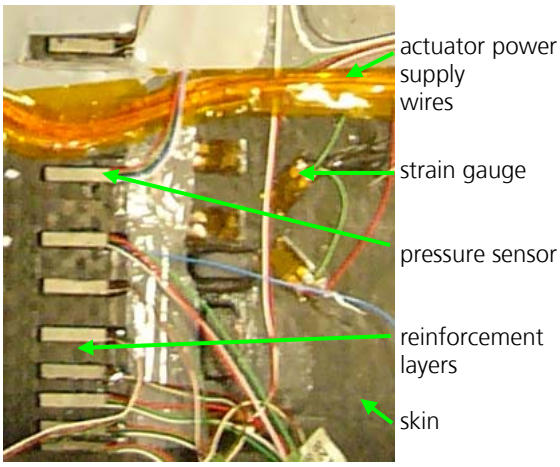


Figure 23: Detail X; installed sensors

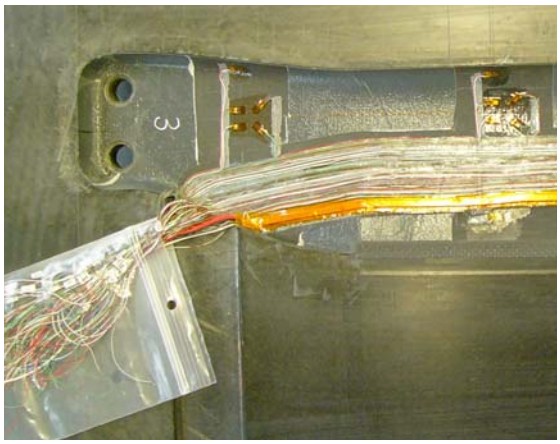


Figure 24: Grommet on the blade root

Main parts of the inner structure of the blades are made of glass fibre and the fames which support the flap actuation system are made of carbon fibre. The carbon frame consists of eight separately manufactured parts which are glued together. Spars and frames are made of fibre stripes and had to be milled to obtain the final shape.

The silver pipes visible in **Figure 25** are necessary to pass the wires from the Hall sensors and the external pressure sensors that were afterwards installed, and the flap pressure sensors from the flap area to the actuator slot where the wires are connected. On the left side of **Figure 25** the spar and the frame are already bonded.

During the assembly of the blades a various number of additional composite layers and reinforcement stripes made of carbon or glass were installed. **Figure 26** shows the root area of a blade during the layering with the spar. The red tape covers wires and avoids that glue clots the wires.

After applying the layers the cavities are filled with foam and a dummy flap and a dummy flap driving system (covered with foam) are installed as visible in **Figure 27**. The latter uses as positioning device of the blade in mould. The last step of the blade assembly is to cover all parts with glue film and to close the blade with the second skin lying in its mould.

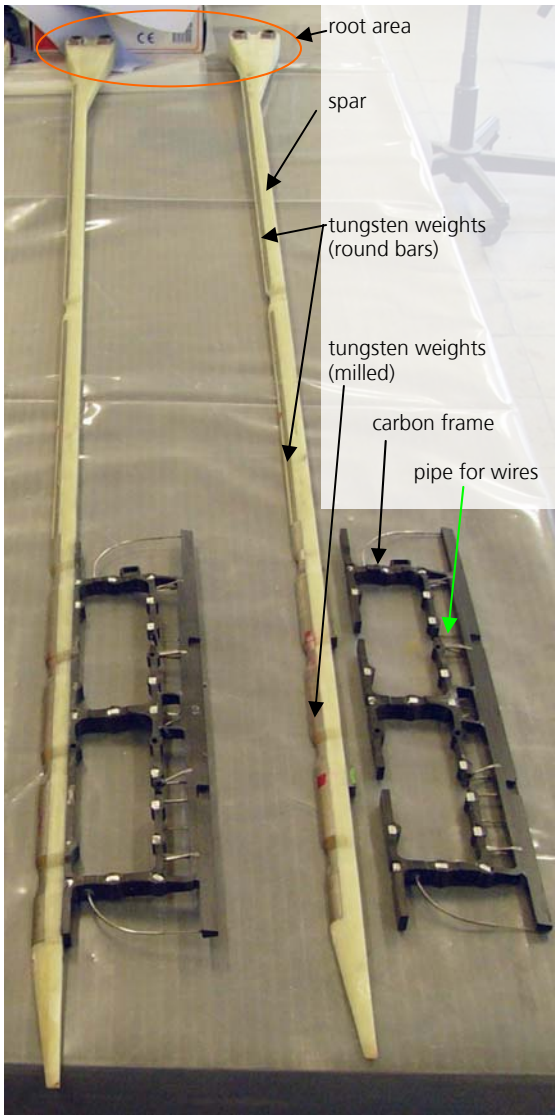


Figure 25: Milled spars and frames

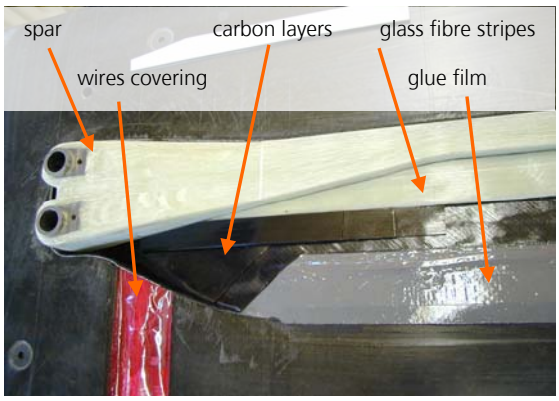


Figure 26: Blade assembly



Figure 27: Blade assembly

Figure 28 shows the blade right before the curing in the oven. Upper and lower moulds are closed using a lot of screw clamps.

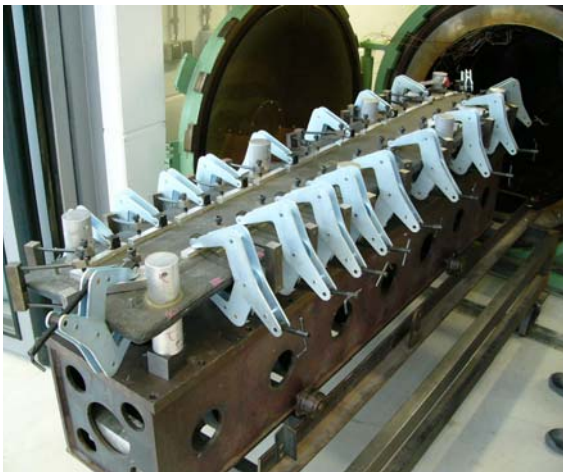


Figure 28: Blade assembly

The final curing process took for four hours at 120°C in our case in addition to heating up and cooling down time.

Thereafter the actuator maintenance cutaway, cavities for the Hall sensors, external installed pressure sensors and the holes for the flap fastening had to be milled and all additional sensors, corresponding wires and the actuator power lines had to be installed.

Figure 29 shows the actuator section of a blade without flaps. The actuator power wires, the connectors and the additional sensor wires are visible on the bottom of the actuator slot. The cups (trap door) of the cutaway are made of carbon fibres and some of them are populated with some pressure sensors.

As mentioned in the paragraph "The ABC Project" three different flap and two different actuator positions are to be realized. For each flap position (inboard, middle and outboard) two respectively three exchangeable flap elements are required whereas during the tests only one element on each blade is operating while the other "dummy flaps" do not have a hinge and are fixed. The hinges of the flaps consist of solid hinges made of glass fibres and metallic knee elements which avoid vertical flap movements.

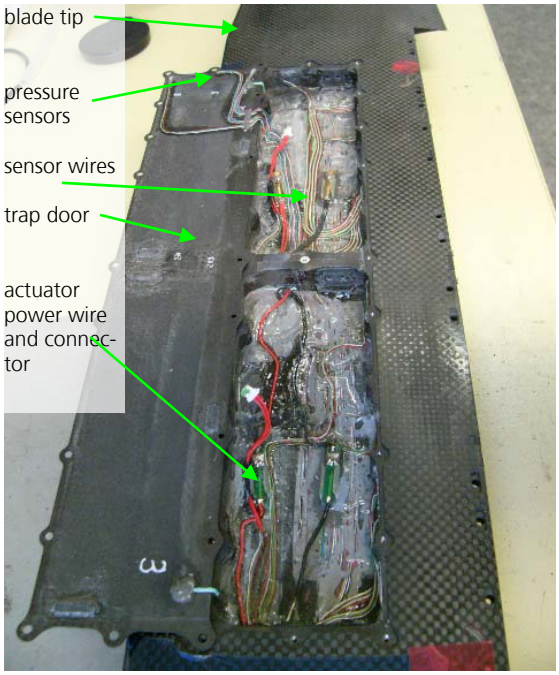


Figure 29: Wiring in the actuator area

Figure 30 shows the flaps respectively the fixed flap elements of two flap configurations (most inboard and middle).

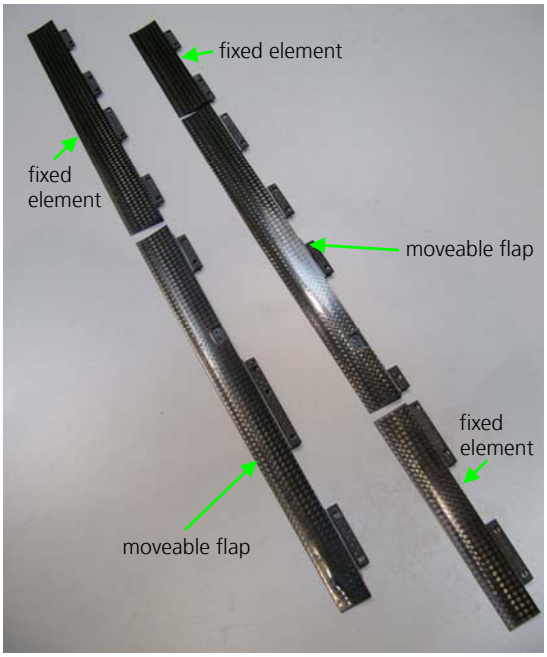


Figure 30: Two flap configurations

Figure 31 deals with the most outboard flap position and the installed flap driving system.

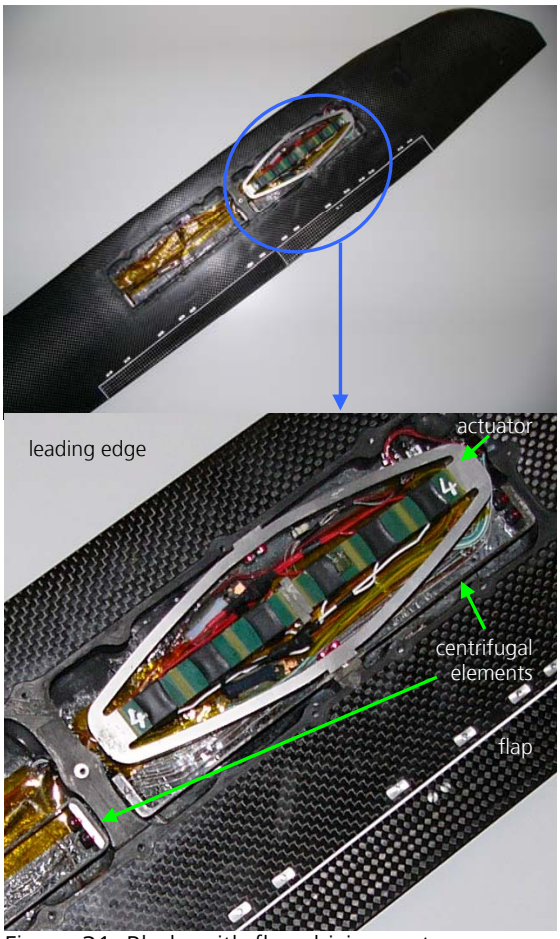


Figure 31: Blade with flap driving system

Tests

The first wind tunnel test will take place in October this year in Modane. A second test is envisaged for Mai 2006 in DNW. Presently the preparations for the Modane test are in full activity. Among other things pressure sensors, strain gages and Hall sensors have to be calibrated, the flap driving system has to be trimmed and the flap controlling has to be tested. A preliminary test of flap control at reduced rpm with multi-harmonic input signal (in hover, so all blade flaps should be in phase. In forward flight they will be shifted by 90deg from blade to blade). As visible in **Figure 32** the blade-to-blade differences in flap deflection are marginal.

Conclusion

The design of ABC rotor blades was very sophisticated mainly because of the implementation of a flap actuation system allowing three flap configurations and because of the high level of instrumentation concerning pressure sensors and strain gages. The manufacturing of prototype blade allowed ONERA and DLR to improve the different steps of manufacturing process.

The series blades were successfully built by DLR. The different lab tests performed in each organization showed that the structural characteristics of the prototype and series blades can be considered as being in very good agreement with the calculations.

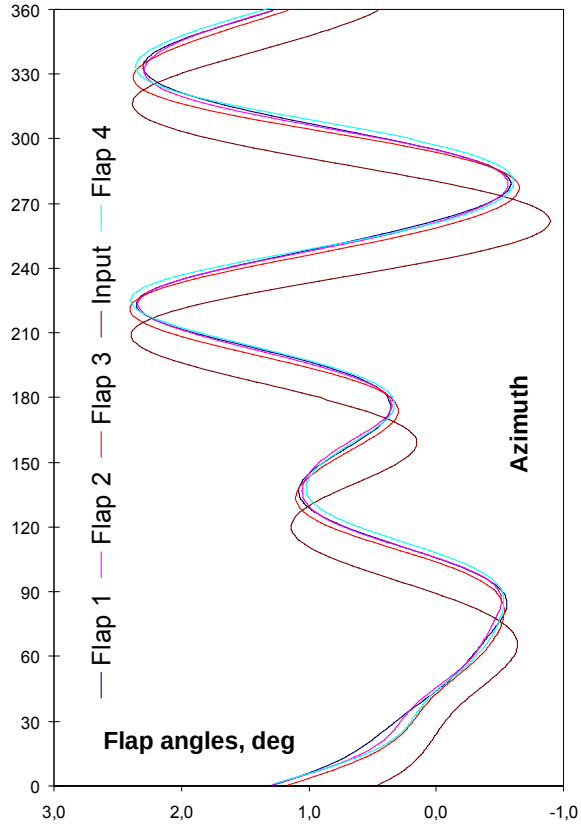


Figure 32: Comparison of flap angles with input

Despite of flap performances slightly lower than those expected, tests of the flap-equipped blades are planned to be held in both S1MA and DNW wind tunnels, respectively focused on the dynamic and acoustic objectives of the project.

References

[1] P. Leconte, H-M. des Rochettes, 'Experimental assessment of an active flap device', 58th Annual Forum of the AHS, Montreal, Canada, 2002

[2] H-M. des Rochettes, P. Leconte, J.L. Petitniot, 'Experimental Assessment and Further Development of Amplified Piezo Actuators for Active Flap Device', Actuator 2002, Bremen, Germany, 2002

[3] M. Kleineberg, A. Pabsch, C. Siegle, "Ermittlung und Charakterisierung der Prozeßparameter eines weiterentwickelten RTM-Verfahrens", Braunschweig, DLR-IB 131-95/34, 1995

[4] B. Enenkl, V. Klöppel, D. Preißler, P. Jänker, "Full Scale Rotor with Piezoelectric Actuated Blade Flaps," 28th European Rotorcraft Forum, Bristol, England, 2002